# Session H

IEEE Transactions on Nuclear Science, Vol. NS-29, No. 6, December 1982

# ELECTROMAGNETIC EMISSION FROM CHEMICAL EXPLOSIONS

V.A.J. van Lint
Mission Research Corporation
5434 Ruffin Road
San Diego, California 92123

## ABSTRACT

EM measurements were made for 60 explosions ranging in mass from 0.01 to 345 kg. Sensors sensitive to broadband LF and narrow-band VHF and UHF were employed. Early time and late time signals are correlated with physical phenomena at the explosion.

## INTRODUCTION

The emission of electromagnetic pulses from chemical explosions was demonstrated almost 30 years ago (Ref. 1-3). An explosion near the earth produces a vertical electric dipole moment that varies on a millisecond time scale (Ref. 4-10). It is thought to be the result of charge separation at the explosion-products/air interface and the asymmetry produced by reflection of the shock from the earth (Ref. 11). The frequency of this signal is consistent with the time scale of the hydrodynamic development of the fireball.

Higher frequency signals in the VHF and UHF bands have also been observed (Ref. 12). Some of these have been associated with the fragmentation of the metal cases enclosing explosives. Others have attributed electric signals to piezo-electric effects in dielectrics (Ref. 13).

## EXPERIMENTAL EQUIPMENT

The experimental setup involved the explosive device with its firing cable, close-in current measurements, a variety of receiving antennas, detectors and amplifiers, and recorders.

### EXPLOSIVE DEVICE

The explosives tests were conducted by the University of California Livermore Laboratory (UCLL) and by Sandia National Laboratory in Albuquerque (SNLA). High explosive (HE) charges size varied from .01 to 345 kg. The configuration varied from simple center-detonated bare spheres to metal encased aerial bombs. The spherically symmetric explosions were supported from an overhead cable at 6-10 m above the ground. Most of the remaining devices were supported on a wooden stand 2 m above the ground. A few were placed on the ground. All devices were connected to a capacitor discharge unit (CDU) by a coaxial firing cable.

### CLOSE IN MEASUREMENTS

On many of the shots the bulk current on the firing cable was monitored with a current probe. On a few shots an insulated 0.6 x 1.3 m Al sheet was placed on the ground near the device. The net current flow to the sheet was measured by a current probe or a 50 Ohm terminated cable. A vertical monopole was also placed at ≈30 m from the device on some shots. Interference was minimized by enclosing the signal cables from the sensors in a 140 m long Al conduit to the recording station.

### ANTENNAS

Most of the RF measurements were performed at a distance of 140 m or 200 m from the detonation. Three types of antennas were used during this test series:

1) 2 m tall monopole. During the early portion of the experiments this was a fiberglass reinforced wire antenna, i.e., an automobile whip. During the later measurements a 1/4" diameter steel rod was used to eliminate impulsive signals produced by flexing of the fiberglass.

2) A log-periodic antenna Hy-Gain electronics Model LP-109. It has a gain of 8 dB, relatively constant over the frequency band from 100 to 1100 MHz and an impedance of 50 Ohms. During the UCLL experiments it was used with a splitter for narrow band 170 and 700 MHz channels.

3) 1.7 m diameter UHF parabolic antennas, Model P5. For most of the measurements this antenna was used to detect fields at 470 MHz. It has a rated gain of 15 dB and an impedance of 30 Ohms. It was also used for 190 MHz and 700 MHz signals during the SNLA experiment.

4) A vertically oriented half-wave dipole with reflector tuned for 57 MHz.

### DETECTORS AND AMPLIFIERS

Although some attempts were made to measure signals with wide-band instrumentation channels, almost all useful data were the result of narrow-band measurements. Gain stability was sacrificed to achieve high sensitivity. This was achieved inexpensively by buying commercial TV tuners and video-amplifiers modified as follows for this application:

1) The AGC loop was opened at maximum gain.
2) The detected video output was connected to an op-amp type amplifier.
3) A 10 μs integrator was incorporated in the amplifier chain to provide good display of the sharp pulses that were being observed.

With the AGC loop opened the video amplifier was operating essentially as a grounded-emitter amplifer without feedback. Therefore, the gain was dependent on a variety of circumstances, including temperature and ageing of the transistors. Since accurate measurements of the absolute power were not considered high priority, this was considered an acceptable instrumentation method. Once the signals became detectable however, the instability of the amplifier caused serious difficulties in calibration and subsequent data analysis. The band width of these receivers is ±3 MHz.

The receiver-amplifier combinations were calibrated periodically by inserting into them a known RF power from a Wavetek Model 2002 A sweep signal generator and observing the signal on the oscilloscope connected to the output of the recorder channel. Only a few such calibrations were performed during the UCLL test series. During the SNLA test series

0018-9499/82/1200-1844$00.75©1982 IEEE

this type of calibration was performed at least twice a day and on some occasions as frequently as four times a day. It was during these measurements that the change in gain during the course of the day, presumably as the temperature increased, was observed. Retrospectively, these changes were applied to both the UCLL and SNLA data, assuming that the trend of the amplifier gain from the cooler early morning to the hot late afternoon was representative both at Albuquerque and Livermore.

The gain of the system, consisting of the propagation path from the device explosion to the antenna location and the antenna connection to the impedance of the receiver was checked twice during the SNLA experiments by placing a quarter wave monopole radiator at ground zero and applying a known power from an RF signal generator. The signal recorded by this means on the oscilloscope was then divided by the receiver gain (measured approximately 1 hour later) to evaluate the effective gain of the antenna. This procedure is also subject to considerable uncertainties. The propagation path between the explosion and the receiver is not free space: it is over a conducting ground and the difference in path length between the direct line of sight and waves scattered from the ground are comparable to the wave length of the radiation being measured. Therefore, it must be assumed that the absolute calibrations are extremely crude and may depend considerably upon the exact position of the RF source, as well as the history of the receiver system.

In the data to be presented we must assume that there is an uncertainty of a factor of 3 in the calibration of the receiver and maybe additional uncertainties due to the nature of the propagation path between the source and the antenna. There is evidence from some of the data that there are other systematic discrepancies between the UCLL and the SNLA data. One obvious cause for this is the use of the log periodic antenna for the 170 and 700 MHz channels at UCLL as distinct from the use of parabolic antennas for the corresponding channels at SNLA. The antenna efficiency used for the UCLL calculation is a theoretical one and is not based upon direct measurements, as in the SNLA data.

The use of the parabolic antenna for the 700 MHz channel produced a distinct improvement in sensitivity during the SLA experiments. Unfortunately the use of the parabolic for the 190 MHz data channel was a mistake; the log periodic or a half-wave dipole cut for resonance at 190 MHz would have been a better choice.

Finally, the intermediate channel was operated at 170 MHz during the UCLL experiments and 190 MHz during the SNLA experiments. This change was required because a TV transmitter located on the Sandia Crest looking directly at the backside of our antenna produced a very large interference at 170 MHz.

## RECORDING AND DATA PROCESSING

Each data channel was displayed on one or more oscilloscopes (sweeping at 10 μs/div or slower) and one channel of FM tape recording (432 kHz center frequency, 80 kHz information bandwidth). Oscilloscope photos were digitized manually. Tape records were digitized automatically at an effective sample pacing of 5 μs using reduced speed playback, analog-to-digital convertor, digital processor and digital tape recorder. The resulting data were then normalized by calibration factors, and subjected to baseline restoration and noise suppression procedures to produce time histories of effective RF power emitted by the explosion.

# EXPERIMENTAL RESULTS

We attempted to identify the causes of various signals by performing measurements on configurations of gradually increasing complexity. These included:

1) CDU, firing cable, and exploding bridge wire (EBW) only.
2) One or more detonators.
3) Detonator, small HE cylinder, metal plate.
4) Suspended center-detonated spherical HE charges; a) bare
   b) metal cases
5) Near-ground cased charges.

## SINGLE TEST CONFIGURATIONS

Figure 1 presents oscilloscope photos of signals recorded on oscilloscopes from two EBW shots (B-18 and B-20). The actual signal is a sharp pulse ocurring at the estimated trigger and cable delay of 12 μs (there is an indication of a double pulse on B-20 at 57 and 170 MHz). The 10 μs decay is produced by the integrators used to make the pulser apparent at slower sweeps and on tape.

Figure 2 presents the signals observed from six detonators placed on a plastic ball. In addition to the EBW signal at "0" time a large pulse signal is seen at all frequencies at 18 μs. The tape records also reveal a pulse at 620 μs in the vertically polarized 470 MHz channel.

A slightly more complex configuration consisted of a detonator at one end of a 1.3 cm long HE cylinder with a thin steel plate at the other end. The resulting signals are shown in Figure 3. The broadband pulse appeared at 13 μs, which is estimated to be slightly before arrival of the detonation wave at the steel plate.

The significance of these results are presented in the discussion section.

## SUSPENDED SPHERICAL EXPLOSIONS

Bare, center-detonated spherical charges exploded away from the ground emitted a few pulses at eary times ($\lesssim$ 100 μs) similar to those shown in Figures 2 and 3. Significant RF bursts occurred at 1 to 5 ms, for yields of 9-18 kg. There is evidence that even a small amount of nearby material (e.g., looping the firing cable past the device) can increase the amount of early-time emission.

Adding an 18 kg steel case around an 18 kg HE charge produces a strong burst of UHF radiation at 100-500 μs, as shown in Figure 4. Emissions at later times (< 1 ms) were still present, but subdued compared to the bare charges. An 18 kg uranium case produced even higher RF power at 100-600 μs, and an intense burst at 33-40 ms, as shown in Figure 5.

## NEAR GROUND SHOTS

Figures 6 and 7 illustrate the RF emission from HE spheres with 70 kg steel cases, and HE masses of 70 and 354 kg, respectively, fired near the ground (2.4 m and 0.4 m, respectively). Both shots exhibit the onset of intense radiation at 200 μs. The larger charge produced more intensive and persistent radiation.

One 20 kg HE cylinder incorporated 20 kg of steel balls within the HE charge for comparisons with steel cased HE configurations. Instead of the 100-200 μs onset of RF radiation, characteristic of metal cased devices, this shot produced a much less intense burst at ≈500 μs.

## CURRENT MEASUREMENTS

No significant net bulk current (< 20 mA) was measured on the firing cable during these shots. There is some evidence of small (≈20 mA) high frequency current spikes occurring during some RF bursts, but these are likely to be due to interference.

During a shot of an 18 kg HE sphere with a 3.6 kg Al case, the current to an insulated Al sheet on the ground was measured and is shown in Figure 8. The negative pulse at 2.7 ms transferred $\approx 2.5 \times 10^{-7}$ Coul. If it's due to a fragment impact, the fragment velocity was ≈200 m/s, a reasonable value. The noisy waveform starting at 7 ms probably coincides with arrival of the air shock at the Al sheet. After recovery the Al sheet exhibited two holes of 1-2 cm diameter, one of < 1 cm diameter and three small dents. It's likely that one of the larger holes was produced by the fragment that carried the measured charge. No RF pulse was observed at 2.7 ms.

## VLF MEASUREMENTS

Monopole antennas at 35 m and 140 m measured the derivative of the vertical electrical field. Sample results from integrating these records to deduce the electric fields are shown in Figure 9. Within the calibration accuracy these fields scale with $1/R^3$, as expected. These signals occur before arrival of the air blast at the sensors.

When the device was suspended at > 7 m above the ground, the monopole signals were undetectable, except for a later time signal from a large charge.

## DISCUSSION

The zero time signals observed in these experiments, mostly at 57 MHz, are most likely due to EM radiation from the firing cable. The finite transfer impedance of the braid-shielded coax cable allows a significant field to be generated externally.

The monopole signals confirm that the region around a chemical explosion contains large electric fields. The field is detectable externally only after an asymmetry is introduced by shock reflection from the ground. An estimate of the effective dipole movement in the source from the data in Figure 9 yields:

$$P = 4\pi R^3 E = 3.0 \times 10^8 \text{ V m}^2$$

the volume within the air shock at ≈10 ms is ≈3000$m^2$. Thus the average electric field within this volume is $\approx 10^5$ V/m; of course, a larger field (up to air breakdown at $\approx 3 \times 10^6$ V/m) could be excited within a smaller volume.

Thus, there is good evidence that the fireball and air shock regions around a chemical explosion contain large radial electric fields. Frequents traversing this region can become charged, as shown by Figure 8. The charge may be limited only by air breakdown at the fragment's surface. For the data in Figure 8, the electric field at the surface of a sphere radius R(m) is

$$E(V/m) = \frac{Q}{4\pi\varepsilon_o R^2} = 2 \times 10^3/R^2$$

Thus, the breakdown field of $3 \times 10^6$ V/m would be achieved with a fragment radius of 2.5 cm. Actually, it's difficult to achieve agreement between the minimum value and a maximum hole size of 2 cm in the Al sheet unless the fragment was very elongated.

It's thus likely that much of the RF radiation is produced by electric sparks in detonation products and from case fragments. The characteristic RF bursts produced by metal cased HE charges starting at 100-200 μs occurs after the case has fragmented and while explosion products are streaming through the spaces between the fragments. Later emissions (> 1 ms can be due to interactions of HE products and charged particles with other nearby materials (e.g., firing cable, support structure, and ground). They appear to require a minimum energy density in the explosion products. For a given HE yield the late time signals appear to decrease with increasing case mass, probably because the accelerating the case material extracts energy from the HE products. The intensity and persistence of late time signals increases with increasing HE yield.

These trends do not explain the intense burst produced by a uranium cased HE charge at 33-40 ms. It could be a one-time fluctuation (i.e., there is considerable variation in the RF radiation history for apparently identical shots). Possibly, it's associated with the pyrophoricity of uranium.

## ACKNOWLEDGEMENTS

The author gratefully acknowledges the assistance of the following:

The staffs of the UCLL and SNLA for providing and firing the devices and furnishing recording instrumentation.

Mr. W.N. Johnston, and Mrs. W. Carr of MRC for instrumentation support and data processing.

Convair Data Lab for Digitizing the tape data.

## REFERENCES

1. Kolsky, H., "Electromagnetic Waves Emitted on Detonation of Explosives", Nature 173, 77 (1954).

2. Takakura, T., "Radio Noise Radiated on the Detonation of Explosives," Publ. Asr. Soc. Japan 7, 210 (1955).

3. Koch, B., "Emission of Short Electromagnetic Waves During Explosive Processes," Compte rendues de l'Acd. des Science 248, 2173 (1959).

4. Anderson, W.H., and C.L. Long, "Electromagnetic Radiation from Detonating High Explosives," J. Appl. Phys. 36, 1494 (1963).

5. Gorshunov, L.M., G.P. Kononenko, and E.I. Sirotinin, "Electromagnetic Disturbances Accompanying Explosions," Soviet Physics JETP 26, 500 (1968).

## REFERENCES (Concluded)


6. Gertsenshtein, M.E., and E.I. Shirotinin, "The Nature of the Electrical Impulse in an Explosion," Ah Prikl Mekh Tekhm Fiz., 11, 72 (1970).

7. Boronin, A.P., V.A. Vel'min, Yu. A Medvedev, and B.M. Stepanov, "Experimental Study of the Electromagnetic Field in the Near Zone of Explosions Produced by Solid Explosives," Zh. Prikl. Mekh. i Tekhn, Fi., 9, 99 (1968).

8. Boronin, A.P., Yu. A. Medvedev, and B.M. Stepanov, "Electrical Pulse from the Pulsations of a Volume of Explosion Products from a Charge of High Explosive," Soviet Physics-Doklady, 17, 925 (1973).

9. Boronin, A.P., Yu. A. Medvedev, and B.M. Stepanov, "Generalized Electrical Pulse and Dissipation of Dynamics of High Explosive Charge Explosion Products," Combustions, Explosions and Shock Waves, 9

10 Walker, C.W., "Observations of the Electromagnetic Signals from High-Explosive Detonation," Lawrence Radiation Laboratory Report, University of California, UCRL-72150, (1970).

11 Wouters, L.F., "Implications of EMP from H.E. Detonation", Lawrence Radiation Laboratory Report, Univ. of California, UCRL-72149, (1970).

12. Trinks H., "Electromagnetic Radiation of Projectiles and Missiles During Free Flight, Impact and Breakdown: Physical Effects and Applications," in 4th International Symposium on Ballistics, Monterey, California, 17, 18, 19 October 1978; published by American Defense Preparedness Association, Washington, D.C. (1978).

13. Hayes, B., "The Detonation Electric Effect", Jour. of Applied Physics 38, 507 (1967).


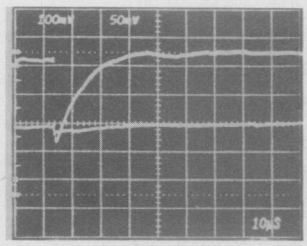

B-18
57 MHz (upper trace)
470 MHz Horizontal
(lower trace)

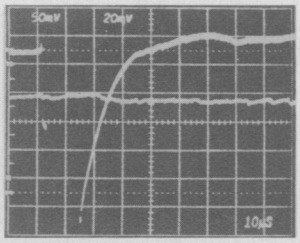

B-20
57 MHz (upper trace)

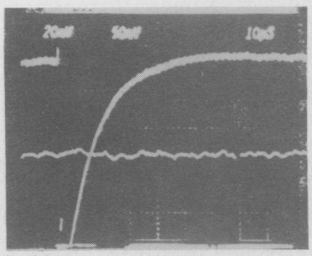

B-20
170 MHz (upper trace)

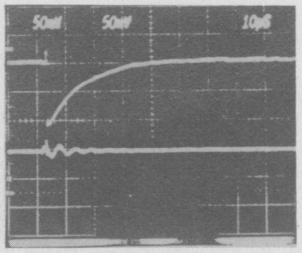

B-20
470 MHz Vertical
(lower trace)

Figure 1. Pulses from EBW.

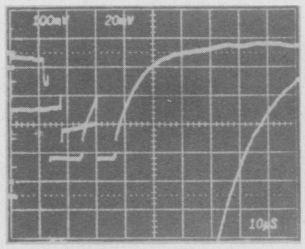

57 MHz (upper)
470 MHz Horizontal
(lower)

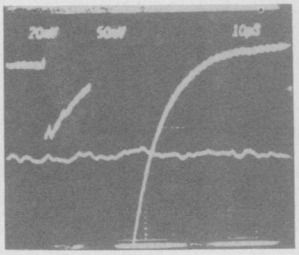

170 MHz (upper)

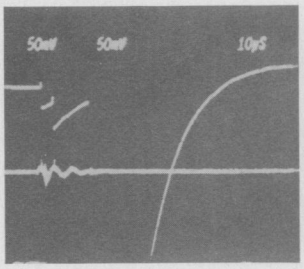

470 MHz Vertical
(upper)

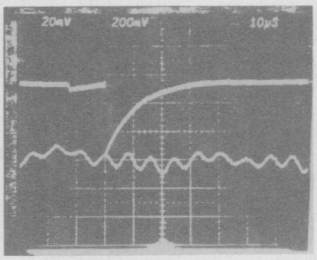

700 MHz (upper)

Figure 2. K-80 signals. 6 detonators on a beach ball (MIL-CDU firing set).

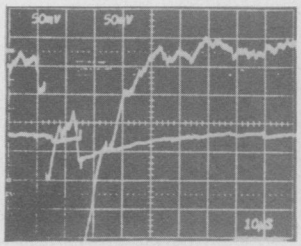

57 MHz (upper)
470 MHz Horizontal
(lower)

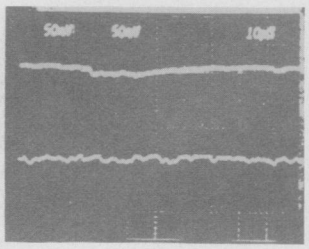

170 MHz (upper)

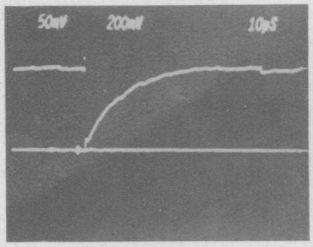

470 MHz Vertical
(upper)

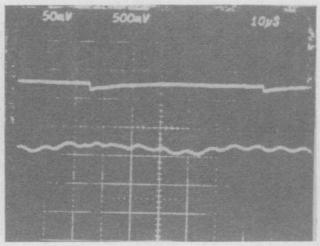

700 MHz (upper)

Figure 3. K-78 signals. HE cylinder with steel plate.

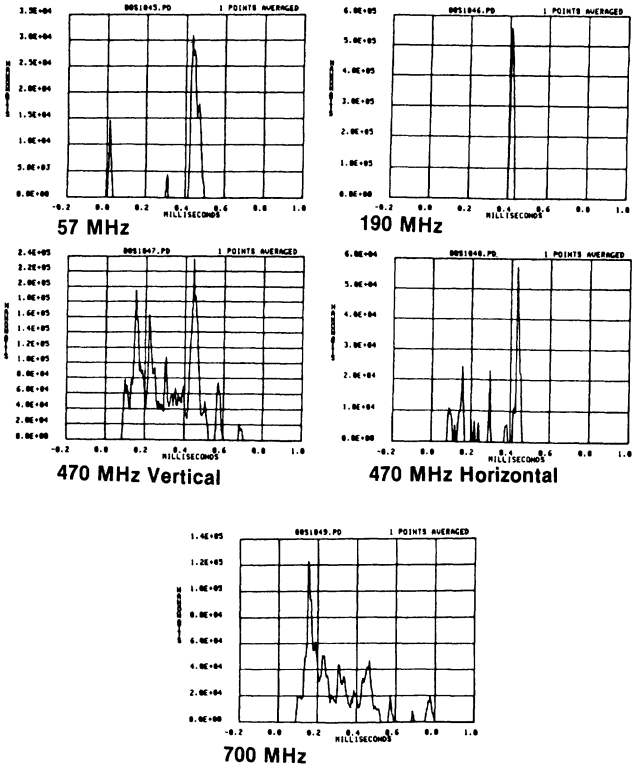


Figure 4. S-10 RF power.

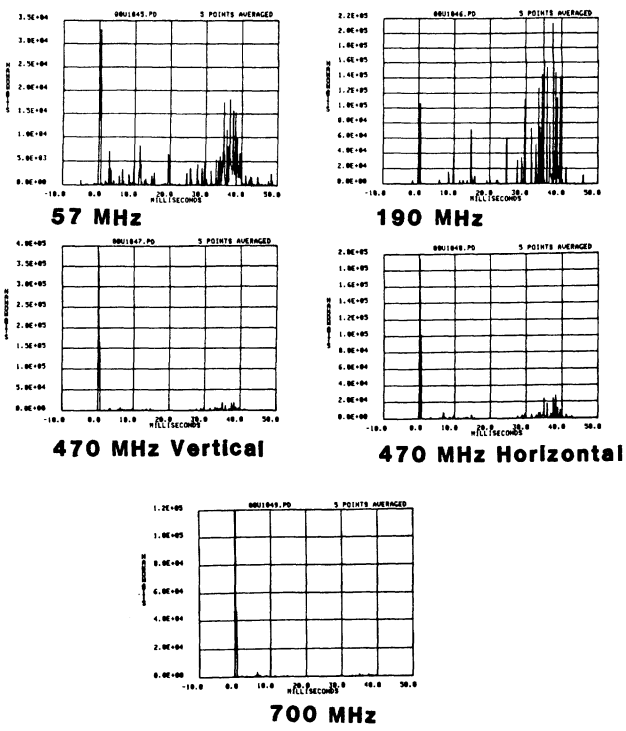


Figure 5. U10 RF power.

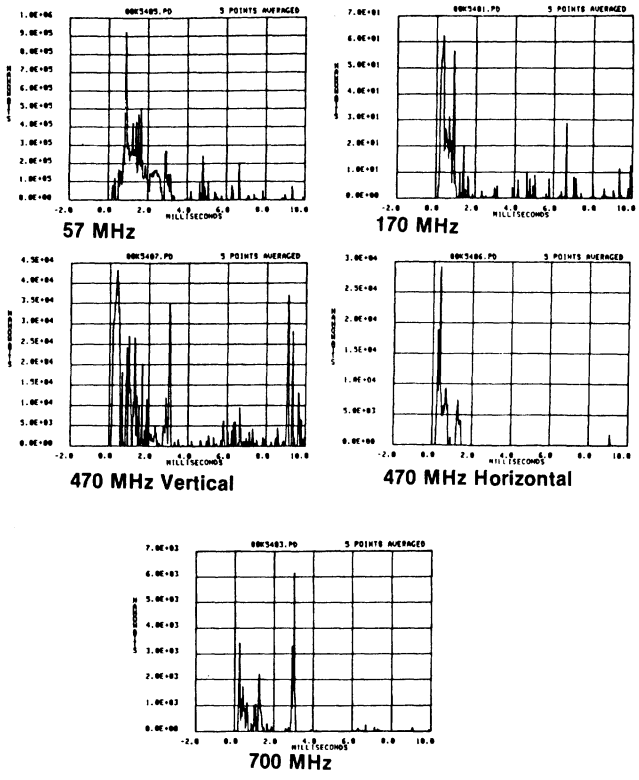


Figure 6. K54 RF power.

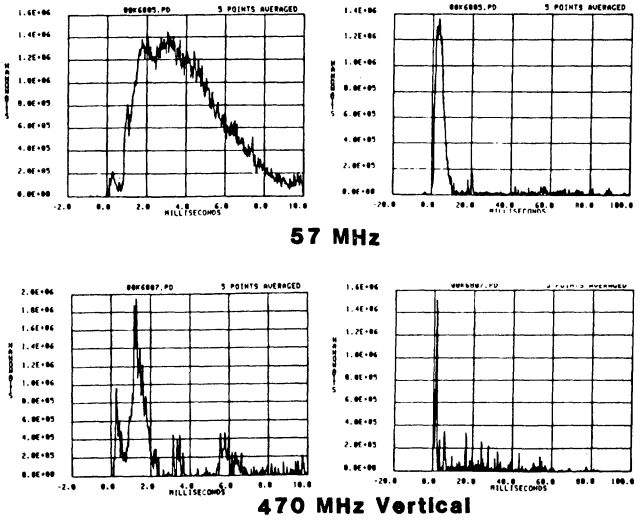


Figure 7. K68 RF power.

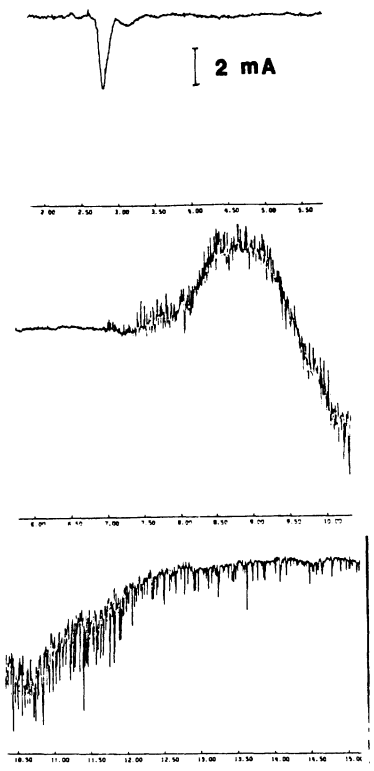


Figure 8. A2 plate current (plate on ground).

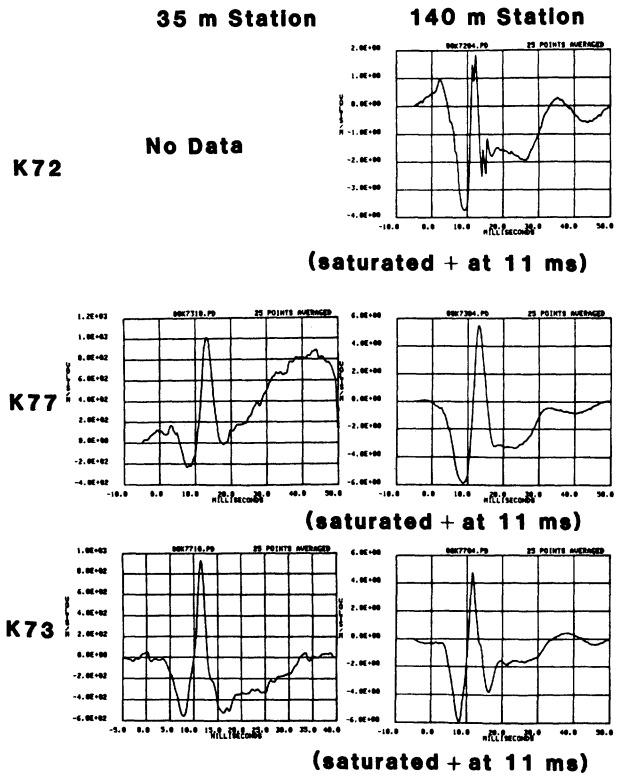


Figure 9. Monopole signals; 46 kg cylinders.